Inverting the Swelling Trends in Modular Self-Oscillating Gels Crosslinked by Redox-Active Metal Bipyridine Complexes

Michael Aizenberg, Kosuke Okeyoshi, and Joanna Aizenberg**

The developing field of active, stimuli-responsive materials is in need for new dynamic architectures that may offer unprecedented chemomechanical switching mechanisms. Toward this goal, syntheses of polymerizable bipyridine ligands, bis(4-vinylbenzyl)[2,2′-bipyridine]-4,4′-dicarboxylate and N4,N4′-bis(4-vinylphenyl)-2,2′-bipyridine-4,4′-dicarboxamide, and a number of redox-active Ruthenium(II) and Iron(II) complexes with them are reported. Detailed characterizations by NMR, Fourier transform infrared spectroscopy, high-resolution mass-spectrometry, X-ray, and cyclic voltammetry show that the topology of these molecules allows them to serve as both comonomers and crosslinkers in polymerization reactions. Electronic properties of the ligands are tunable by choosing carboxylate- or carboxamido-linkages between the core and the vinylaryl moieties, leading to a library of Ru and Fe complexes with the M(III)/M(II) standard redox potentials suitable for catalyzing self-oscillating Belousov–Zhabotinskii (BZ) reaction. New poly(*N*-isopropylacrylamide)-based redox-responsive functional gels containing hydrophilic comonomers, which have been prepared using representative Ru bpy complexes as both a crosslinker and redox-active catalyst, exhibit a unique feature: their swelling/contraction mode switches its dependence on the oxidation state of the Ru center, upon changing the ratio of comonomers in the hybrid gel network. The BZ self-oscillations of such crosslinked hydrogels have been observed and quantified for both supported film and free-standing gel samples, demonstrating their potential as chemomechanically active modules for new functional materials.

1. Introduction

Polypyridine ligands and their transition metal complexes have been an active area of research for several decades now.[1,2] Ruthenium complexes with polypyridine ligand core, in particular, have occupied a significant place in this body of work, in big part due to the fact that they have been recognized to be useful in a wide variety of applications, which rely on their chemical stability, as well as a unique combination of photochemical, electrochemical, and photophysical properties. Among many potential applications that have emerged over the years, some recent examples include mononuclear water oxidation catalysis,[3] light-emitting electrochemical cells,[4] photoredox catalysis coupled with organocatalysis,[5] light-activated anticancer drugs,[6] and dye-sensitized solar cells.[7,8] Interest in integrating these valuable properties of polypyridine metal complexes into materials and devices gave rise to research in bipyridine-containing polymer ligands, as well as metallopolymers, coordination polymers, supramolecular polymers, and crosslinked polymer gels containing bipyridine moieties.[9] The targeted applications and research areas include, among others, electroluminescent, electrochromic, and photoluminescent materials,[9b,10,11] sensors,[9b,12] and chemomechanically active self-oscillating gels.[13–16]

Interdisciplinary field of development and application of stimuli-responsive materials continues to attract significant attention of materials scientists.[17] Within the framework of our on-going research in hybrid, responsive, and autonomous materials, which have chemomechanical or mechanochemical transformations at their core, we became interested in redox-active polypyridine complexes, especially those of ruthenium, as catalytic centerpieces of self-oscillating gels, in particular those of Belousov–Zhabotinskii (BZ) type. BZ reaction[18,19] is a sequence of chemical processes, consisting of a metal-catalyzed oxidation of an organic reducing agent (typically malonic or citric acid) by an inorganic oxidant (typically BrO_3^-) that due to an interplay of autocatalytic oxidation steps and generation of an inhibitor in their course (typically bromide ion) results in chemical oscillations, including those clearly visible by eye. To date, almost all work on BZ gels, with not very many exceptions,[20] that were recently reviewed,[21] relies on the ruthenium complex with (4-Me,4′-Vi)-2,2′-bipyridine: $[Ru(bpy)_2((4\text{-Me},4'\text{-Vi})\text{-bpy})](PF_6)_2$.[22] Both the ligand[22–24] and the complex, despite being known for a long time, are relatively difficult to synthesize and purify, which somewhat limits both

Dr. M. Aizenberg, Prof. J. Aizenberg
Wyss Institute for Biologically Inspired Engineering
at Harvard University
60 Oxford Street, Cambridge, MA 02138, USA
E-mail: michael.aizenberg@wyss.harvard.edu; jaiz@seas.harvard.edu
Dr. K. Okeyoshi, Prof. J. Aizenberg
John A. Paulson School of Engineering and Applied Sciences
Harvard University
29 Oxford Street, Cambridge, MA 02138, USA
Prof. J. Aizenberg
Department of Chemistry and Chemical Biology
Harvard University
12 Oxford Street, Cambridge, MA 02138, USA
The ORCID identification number(s) for the author(s) of this article can be found under https://doi.org/10.1002/adfm.201704205.

DOI: 10.1002/adfm.201704205

the access to them and the achievable modularity/tunability of materials systems based on these building blocks. Our goal has been to expand the toolbox of the BZ-active gels, in order to get access to a number of polymerizable catalysts and, potentially, to be able to apply them as modules in hydrogel-actuated integrated responsive systems (HAIRS)—a dynamic, hybrid materials platform composed of an array of skeletal microstructures embedded into and put in motion by a hydrogel muscle.[25–27] We have been exploring the latter for a variety of applications, including control of wettability and flow,[28,29] switching of chemical reactions,[30] and catch-and-release of molecules.[31] With these considerations in mind, we wanted to develop straightforward synthetic approaches to a family of polymerizable bipyridine-type ligands and to their complexes of ruthenium, and other metals, that may find use as catalysts in BZ-active self-oscillating gels and other autonomous systems.

There is a variety of approaches to the synthesis of polymers that contain metal-polypyridine moieties.[32] Depending on the particular target structure, they may include, among others: (i) preparation of ligand polymers followed by metal coordination; (ii) polymerization or polycondensation of metal complex-containing polymerizable/polycondensable molecules; (iii) coordination polymerization using ligands that contain polypyridine moieties on both ends of the same molecule; or (iv) using various metal-catalyzed coupling reactions on strategically positioned reactive groups on the periphery of the monomer complex. Many of these synthetic approaches, however, lead to poor control over the yield and selectivity of the desired reaction, often requiring the chromatographic separation of complex mixtures or a multistep synthesis of well-defined pure monomers and building blocks. Here we report on syntheses of two ligands having 2,2′-bipyridyl-4,4′-dicarboxylic acid core linked through ester or amide linkages to polymerizable and crosslinkable vinylaryl groups and their Ru (II) and Fe (II) complexes. We demonstrate that they can be copolymerized into hydrogel networks that can act as catalysts in functional, hybrid, self-oscillating materials in BZ reaction, both as free-standing and with the HAIRS microstructure arrays embedded in them. Furthermore, we present first examples of the unique behavior of the prepared redox-responsive hydrogel materials that exhibit the switching of the swelling/contraction modes depending on the hydrophilicity of the polymer network.

2. Results and Discussion

2.1. Development of Modular Polymerizable Ru and Fe Complexes and Their Assembly into Hybrid, Redox-Active Metallopolymers, and Gels

2.1.1. Synthesis of Ligands

As primary cores for the ligands, we chose commercially available 2,2′-bipyridine substituted in 4 and 4′ positions with carboxylic groups that can be easily converted into esters or amides. As building blocks for installing polymerizable functions, we chose commercially available 1-(chloromethyl)-4-vinylbenzene and 4-vinylaniline. The straightforward synthetic pathways for the preparation of the two vinyl-bearing ligands are presented in **Scheme 1**a. The presence of vinyl groups in the products **4** and **5** (73% and 88% yield, respectively) is evident from the appropriately positioned and split signals in proton and carbon NMR spectra and the presence of the ester and amide carbonyl groups peaks ($\nu_{C=O}$ = 1720 cm^{-1} in **4** and $\nu_{C=O}$ = 1649 cm^{-1} in **5**) in the Fourier transform infrared (FTIR) spectra (see the Experimental Section and the Supporting Information for details). Additionally, the connectivity in ligands was confirmed by single crystal X-ray structure of **4** as an example (see Figure S1 and Table S1 of the Supporting Information for detailed X-ray data), and the identity of both ligands **4** and **5** was further supported by the high-resolution mass-spectrometry (HRMS) data (see the Supporting Information).

*2.1.2. Synthesis of Ru Complexes with Bipyridine Ligands **4** and **5***

Among the most typical approaches to cationic late transition metal complexes that involve removal of bound halides and replacing them with non-coordinating anions,[33–37] we chose the most simple reaction between *cis*(bpy)$_2$RuCl$_2$ and AgPF$_6$ in methanol,[37] which ensured direct installation of non-coordinating [PF$_6$]$^-$ counterions, allowing us to alleviate the need in additional step of anion exchange. The resulting complex, [(bpy)$_2$Ru(CH$_3$OH)$_2$](PF$_6$)$_2$,[33] reacted smoothly with ligands **4** and **5** and formed in close to quantitative yield the desired products [(bpy)$_2$Ru(**4**)](PF$_6$)$_2$ (**6**) and [(bpy)$_2$Ru(**5**)](PF$_6$)$_2$ (**7**) (Scheme 1b), which were fully characterized by multinuclear NMR, FTIR spectroscopies, and HRMS. The proton and carbon NMR data confirm the presence of the coordinated functionalized bipyridine, along with two unsubstituted bpy ligands. The installed double bonds are retained and are available for polymerization reactions. The presence of ester or amido carbonyls was confirmed by FTIR spectroscopy ($\nu_{C=O}$ = 1719, 1676 cm^{-1}, for **6** and **7**, respectively). Hexafluorophosphate counterions give rise to appropriately positioned and split signal in ^{19}F{^{1}H}-NMR spectrum (δ –70.5 (d, J = 711 Hz) and are also detected in HRMS in a form of [M-(PF$_6$)]$^+$ signals with the expected isotope patterns (see the Experimental Section for details).

The connectivity of complex **6** was characterized by single crystal X-ray structure of its adduct with dichloromethane (**Figure 1** and see Table S1 of the Supporting Information for detailed X-ray results). The structural data show (i) no steric congestion around the Ru center that is positioned in a slightly distorted octahedral coordination formed by six nitrogen atoms: four belonging to two unsubstituted bpy ligands, and remaining two from the ligand **4**, and (ii) the double bonds that are located on the periphery of the complex, far from each other, being readily accessible for polymerization or copolymerization. The complex itself, therefore, is perfectly suited to serve as a comonomer and a crosslinker in a hybrid polymer architecture.

*2.1.3. Synthesis of Fe Complexes with Bipyridine Ligands **4** and **5***

For the synthesis of Fe complexes, a one-step approach was adopted starting from commercially available complex [Fe(H$_2$O)$_6$](BF$_4$)$_2$. The choice of this compound was dictated by the following considerations: (i) this starting material is already

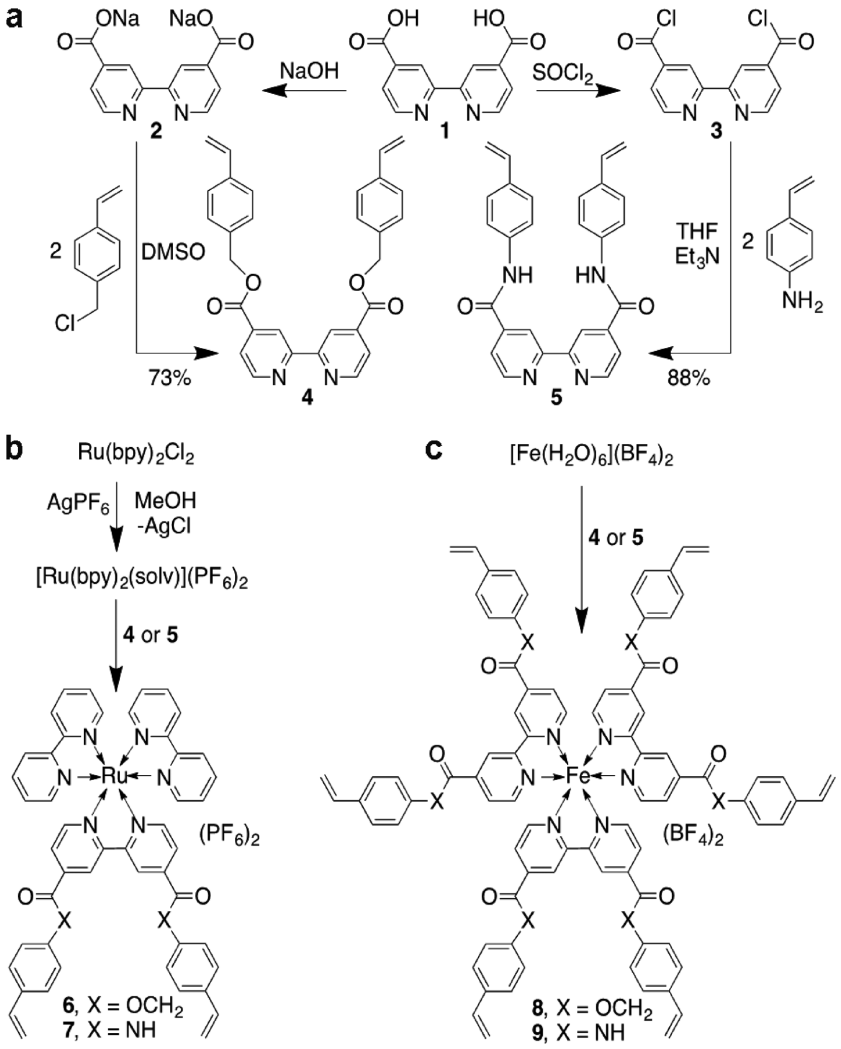

Scheme 1. Synthetic procedures. a) Synthesis of ester- and amido-linked bipyridine (bpy) ligands. b) Synthesis of Ru(II) complexes containing one ester- or amido-linked (vinylaryl) bpy ligand **4** or **5** per metal center. c) Synthesis of Fe(II) complexes containing three ester- or amido-linked (vinylaryl) bpy ligands **4** or **5** per metal center.

a cationic Fe(II) complex with non-coordinating $[BF_4]^-$ anions, so aqua-ligand substitution reactions were expected to be straightforward, and (ii) this starting material does not contain a partly installed bis-bipyridine core. Therefore, we were able to achieve in resulting complexes a highly modular topology with three sets of bpy ligands, each of which having two polymerizable moieties per metal center. The reactions between $Fe(H_2O)_6(BF_4)_2$ and ligands **4** or **5** produced the desired *tris*-substituted Fe(II) complexes **8** and **9** in close to quantitative yields (Scheme 1c).

2.1.4. Modular Approaches to Assembling Redox-Active Metallopolymers and Gels

Ru(II) and Fe(II) complexes **6–9** offer substantial modularity in the composition and structure of various polymers and gels containing these redox-active metal centers. They make possible a number of hybrid polymer architectures, due to the fact that complexes **6** and **7** have two polymerizable vinylaryl groups per metal center, while **8** and **9** have six. Furthermore, with the ability to install ester or amido-linkages, electronic/redox properties of the complexes as well as their hydrolytic stability become additional variable parameters. Within the same or similar architectures and topologies, one can envision additional degrees of freedom that could originate from changing the bipyridine core to the biquinoline one. Doing that would affect the steric situation around the metal center, bringing an additional level of modularity to the synthesis of metal complex-containing polymers and gels with desired reactivities (though not a focus of the current study, as a demonstration of the utility of our synthetic approaches, we prepared biquinoline analogues of ligands **4** and **5** (**10**, **11**) and we report their syntheses and characterization in the Supporting Information).

The measured electrochemical characteristics of complexes **6–9** are summarized in **Table 1**. The M(III)/M(II) reduction potentials have been determined from cyclic voltammograms in 0.10 M $(Bu_4N)ClO_4$ in acetonitrile as electrolyte with Ag/0.01 M $AgNO_3$ in acetonitrile as reference electrode. Redox potential of ferrocene/ferricinium measured under the same conditions was between +84 and +90 mV—very close to the reported value of +87 mV measured against an Ag/0.01 M $AgNO_3$ electrode in 0.1 M $(Et_4N)ClO_4$ in acetonitrile.[38] Further, the potentials were recalculated against saturated calomel electrode (SCE) and standard hydrogen electrode (SHE) as reference electrodes by introducing the appropriate factors: +0.380 V to convert the potentials referenced to ferrocene standard to those referenced to SCE, and +0.244 V to convert the potentials referenced to SCE to those referenced to SHE.[38]

As seen from Table 1, the potentials are sensitive to the type of ligand used: as expected, going within the same metal center series from the more electron-poor ester-functionalized bipyridine ligand **4** to the more electron-rich amidofunctionalized ligand **5**—that is from Ru complex **6** to **7** and from Fe complex **8** to **9**—the oxidation potential decreases.[39] Notably, the magnitude of such reduction is higher for the complexes having higher number of substituted bipyridine ligands: ≈35 mV for **6–7** pair, in which the complexes have just one bis-functionalized bpy ligand each, and ≈90 mV for **8–9** pair, in which all three bpy ligands are bis-functionalized.[39] The absolute value of the potentials measured for Ru complexes **6** and **7**, 1.607 and 1.572 V respectively, fall within the range of potentials reported for (i) the unfunctionalized $[Ru(bpy)_3]^{2+}$, 1.521 V, (ii) a closely related bis-ethyl-ester-functionalized $[Ru(bpy)_2((4,4'\text{-}COOEt)_2\text{-}bpy)]^{2+}$, 1.643 V, and (iii) $[Ru(bpy)_2(4,4'\text{-dimethyl-bpy})]^{2+}$, 1.508 V, electronically

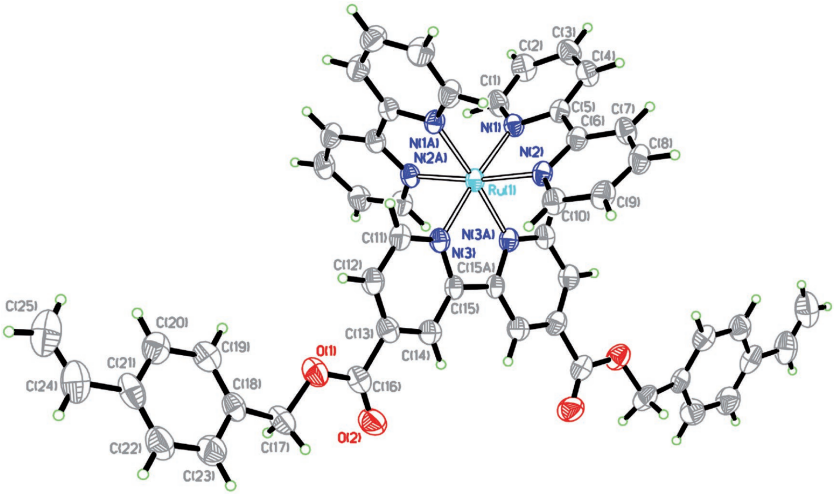

Figure 1. ORTEP view of the X-ray crystal structure of $[(bpy)_2Ru(\mathbf{4})](PF_6)_2 \cdot 0.67\ CH_2Cl_2$ ($\mathbf{6} \cdot 0.67\ CH_2Cl_2$); the dichloromethane molecule and $PF6^-$ anions are not shown; ellipsoids are shown at 50% probability. Note that a metal center is not sterically congested, which ensures the stability of the complex, and that the double bonds are located on the periphery of the structure and are therefore available for polymerization, enabling the complex to act as a crosslinker in polymerized structures.

similar compound to the polymerizable BZ catalyst $[Ru(bpy)_2(4\text{-Me, }4'\text{-Vi-bpy})]^{2+}$.[39]

It has been suggested that for a metal complex to be able to catalyze BZ reaction, it should contain a one-electron redox couple whose standard oxidation potential should fall between 0.9 and 1.6 V.[40] This criterion, though seemingly fairly broad, is nevertheless a useful guideline for selecting candidates for BZ catalysts from a library of transition metal complexes. Of course, the absolute and relative concentrations of the oxidant and the reductant used in the BZ reaction mixture are of importance, too, and they may need adjustment for the best oscillation performance.[40] From the cyclic voltammetry data we obtained for complexes **6–9** and from the comparison of their measured redox potentials to those of known BZ catalysts, it follows that they satisfy the above criterion on both parameters and, therefore, are expected to be suitable catalysts for the BZ reaction.

2.2. Various Swelling Trends and Self-Oscillating Behavior of Metal Complex-Crosslinked Gels

*2.2.1. Hydrogels Based on Poly(N-Isopropylacrylamide) (PNIPAAm) with Complexes **6** and **8** as Crosslinkers*

For the initial series of gel formation experiments, we chose complexes **6** and **8** as they comprise a small, but representative subset from the library of compounds we had at our disposal.

Table 1. Electrochemical Data for complexes **6–9**.

Compound	6	7	8	9
$E_{1/2}(M^{III}/M^{II})$ *V*, vs Fc^+/Fc	0.983	0.948	0.961	0.870
$E_{1/2}(M^{III}/M^{II})$ *V*, vs SCE	1.363	1.328	1.341	1.250
$E^{o\prime}(M^{III}/M^{II})$ *V*, vs SHE	1.607	1.572	1.585	1.494

In particular, they (i) had the same polymerizable ester-linked bipyridine ligand (**4**), (ii) represented two different metal centers (Ru and Fe), (iii) were expected to lead to different types of crosslinked architectures of the gel network (mono-crosslinked and potentially up to *tris*-crosslinked), and (iv) exhibited higher solubility than the complexes with amido-linked ligand **5**. The fabrication schematic and two exemplary architectures resulting from the polymerization of *N*-isopropylacrylamide (NIPAAm) with complexes **6** and **8** are shown in **Figure 2**. As the underlying substrate, we chose micropost arrays arranged in a square lattice and having the following dimensions: (a) on a smaller scale, diameter—1.5 µm, height—10 µm, pitch—9 µm (Figure 2), and (b) on a larger scale, diameter—10 µm, height—100 µm, pitch—25 µm. The latter, larger scale samples of gels were used for detailed, quantitative characterization of the swelling properties and dynamic changes occurring in hybrid gels, and their dependence on the metal redox state and on the gel's composition. The details of the preparation of the micropost array and the preparation of the hydrogels are described in the Experimental Section.

2.2.2. Effect of Network Hydrophilicity on the Swelling Ratio of Metal Complex-Crosslinked PNIPAAm Gels Having Hydrophilic Comonomers

For these studies, we first chose to prepare a series of hybrid PNIPAAm gels with **6**, as the architecturally most simple crosslinker,[14b] and 2-acrylamido-2-methylpropane sulfonic acid (AMPS), as the acidic, highly hydrophilic comonomer, which has been successfully used in some oscillating gel formulations, including the ones that operate under acid-free conditions.[13b,c,f,15a] A larger-scale micropost array used as a substrate was modified with a thin layer of nonadhesive Au/Pd, which allowed us to peel off geometrically well-defined, thin, free-standing square pieces of bulk gel, ideally suitable for studies of their swelling/deswelling behavior (**Figure 3**). Peeling off the microporous gel samples from the substrate was facilitated by the gel swelling that occurred during immersing them in given solutions (see the Experimental Section for details).

With the amount of crosslinker **6** kept at 1 mol%, the monomer mol% ratio NIPAAm:AMPS was varied in four samples as 99:0, 84:15, 69:30, and 0:99. The results of the swelling ratio studies were completely unexpected (**Figure 4**). As seen in Figure 4a, with no AMPS in the gel composition, the swelling ratios of both oxidized and reduced gels are very small and change very little with temperature. The works by Yoshida et al. have proposed and shown experimentally that in the systems where $[Ru(bpy)_3]^{2+}$ is a pendant group, this moiety, in its reduced form, imparts substantial hydrophobicity to the poly(NIPAAm) hydrogel crosslinked by methylenebisacrylamide[13a,c,f] The

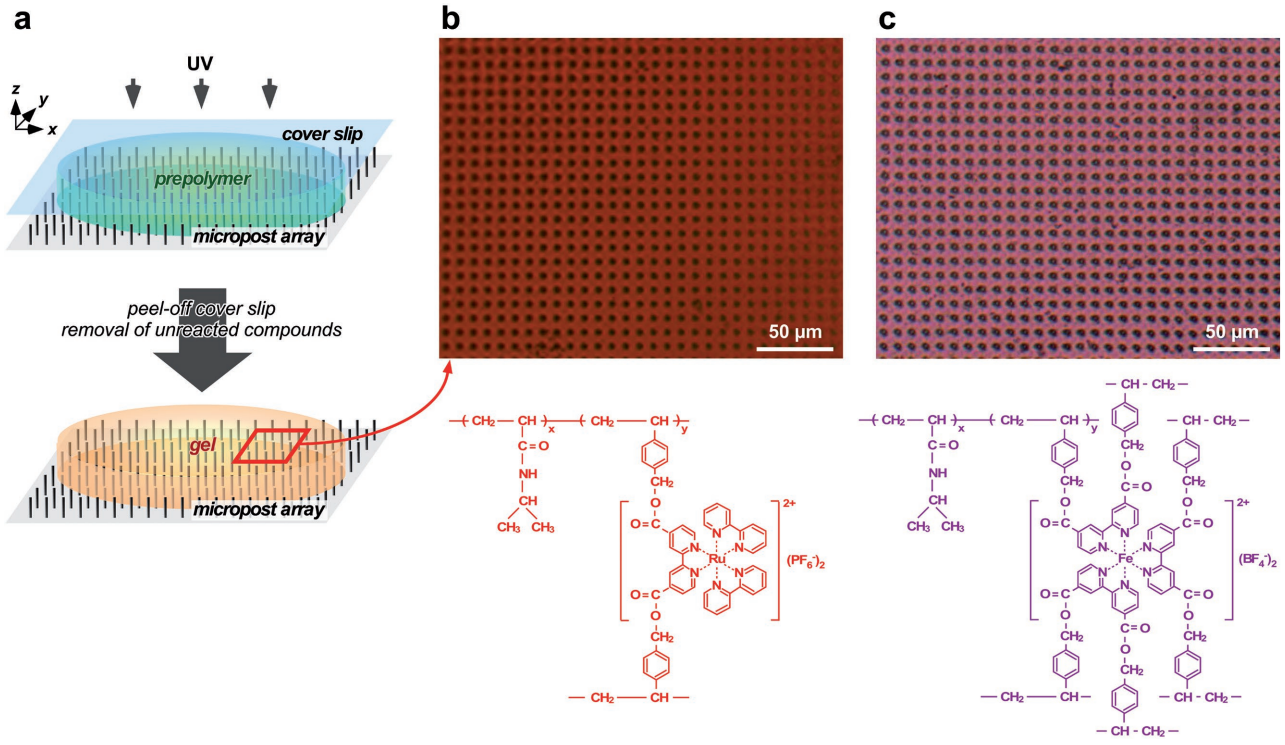

Figure 2. Schematic of fabrication of the gels on microstructures a) and optical microscope images along with respective chemical structures of PNIPAAm gels crosslinked with Ru complex **6** b), and Fe complex **8** c) and integrated with the small-scale microstructure array.

oxidation of the Ru center makes the network less hydrophobic, allowing water to go into the network and swell the gel. The variety of the compositions of such gels with pendant $[Ru(bpy)_3]^{n+}$ moiety, including those that can operate in acid-free conditions[13c,f] and oxidant-free conditions,[13e] all exhibited similar trends in their swelling/contraction behavior: higher hydrophilicity and solubility with oxidation and/or addition of AMPS comonomer into the network and higher hydrophobicity/lower solubility upon reduction and/or without AMPS in the network. The presence of AMPS, together with the oxidation state of Ru center, were shown to participate in a delicate balance of overall gel hydrophilicity affecting (along with the temperature), in a fairly wide range, conditions under which the oscillations were possible.[13c] The gels that we report here not only have the $[Ru(bpy)_3]^{n+}$ moiety as the crosslinker, they also have the metal center coordinated to a substantially more hydrophobic ligand possessing (vinyl)benzyl ester groups. As is apparent from the data in Figure 4, the overall hydrophilic/hydrophobic balance of the gel networks, which have **6** as the crosslinkers, gets even more complicated and not monotonous. This unexpected complex swelling performance is in stark contrast to the well-described behavior of the conventional poly(NIPAAm-*co*-$Ru(bpy)_3$) BZ-active gel, which shows a higher swelling ratio for the oxidized gel than that for the reduced gel. With the introduction of increasing amounts of AMPS, the swelling ratios of oxidized and reduced gels start to diverge and depend quite noticeably on temperature (Figure 4a). Furthermore, there is a unique inversion point between 15 and 30 mol% of AMPS, at which absolute values of swelling ratios of reduced and oxidized gels switch their order: at 15 mol% AMPS, the swelling ratio of the reduced gel is higher than that of the oxidized gel in the studied temperature range, whereas at 30 mol% AMPS, the reverse (and typical) order is observed (Figure 4a).

In order to probe whether the observed inversion of the redox-mediated swelling behavior of PNIPAAm gels is unique to the chosen NIPAAm-AMPS set of comonomers or it is a phenomenon that is more general in nature, we prepared exact same compositions of gels, but used as a comonomer (3-acrylamidopropyl)trimethylammonium chloride (AAPTAC). The same set of experiments measuring the swelling ratio trends of poly(NIPAAm-*co*-AAPTAC) gels showed that the inversion of the swelling ratio occurs for these gels as well (Figure 4b). The inversion point for this comonomer is positioned at 30 mol%.

This signifies that the behavior of the $Ru(bpy)_3$-crosslinked poly(NIPAAm-*co*-AMPS) and poly(NIPAAm-*co*-AAPTAC) gels is distinctly different from that of conventional BZ gels, in which redox-active metal complexes are pendant rather than serving as covalent linkages between the polymer chains. This phenomenon indicates strongly that a typical model that explains the increase in the level of hydration, and hence the swelling, by a simple increase in the charge of the metal center (Ru^{3+} in oxidized state vs Ru^{2+} in reduced state), taken alone, is not operational in this case. We further note that examples of the swelling behavior opposite to the typical trend, i.e., shrinkage of the oxidized rather than reduced forms of gel, was recently reported for pendant Ru complexes in polyacrylamide gels[20] and for Ru-based hyper-crosslinked gels.[14b] The offered qualitative explanation for this phenomenon, when the metal complex served as a crosslinker,[14b] has at its core the reduced mobility of the metal centers in the crosslinking positions (compared to

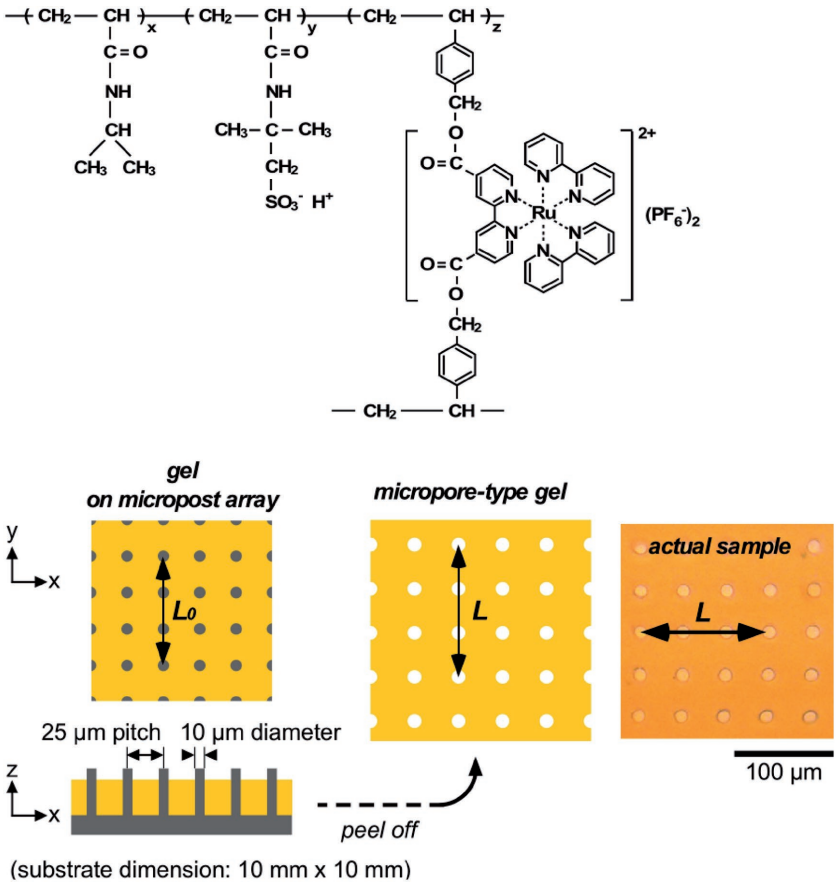

Figure 3. Chemical structure of $Ru(bpy)_3$-crosslinked poly(NIPAAm-*co*-AMPS) gel, schematic of the preparation of free-standing bulk samples for swelling ratio studies and a micrograph of an actual gel sample. By polymerizing the gel on the substrate bearing a square array of microstructures, and by peeling it off, a free-standing sample with a regular array of holes is formed. The swelling/contraction was measured by dividing the distance between the holes in the sample subjected to different conditions (L) by that in the original, not peeled off sample (L_0). For detailed definition of the molar amounts of the comonomers and the crosslinker used see main text and the Supporting Information.

that of the pendant ones in the conventional poly(NIPAAm-*co*-$Ru(bpy)_3$) BZ-active gel) and the resulting need to attract additional counterions into a congested network environment with limited flexibility, ultimately leading to the water expulsion and network collapse.

Importantly, irrespective of whether the earlier studies described the typical or reverse swelling/contraction trend, no inversion of the swelling behavior was reported. The observed inversions in $Ru(bpy)_3$-crosslinked PNIPAAm gels containing hydrophilic comonomers make them, therefore, distinctly different from other redox-active gels, and neither mechanism described above can offer an adequate explanation for the unique switching of the swelling behavior. Some of the above arguments can certainly be applicable for our cases, but there have to be additional factors at play that result in the reversal of the swelling ratio order upon increase in the loading of hydrophilic comonomers (AMPS or AAPTAC) in gel's architecture. Rather, oxidation and reduction events affect substantially the overall conformational arrangement of the poly(NIPAAm-*co*-AMPS) and poly(NIPAAm-*co*-AAPTAC) gel networks leading to different directions in the changes of overall hydrophilicity (and thus of swelling ratios) for the different levels of AMPS or AAPTAC incorporation. This seemingly counterintuitive relationship resembles, in some way, and can be possibly related to the earlier observed phenomenon of sharp discontinuous volume phase transitions of pNIPAAm gels containing ionic sodium acrylate comonomer.[41]

2.2.3. BZ Reaction in Poly(NIPAAm-co-AMPS) Functional Gels Crosslinked by **6**

The highest difference in swelling ratios between oxidized and reduced states of poly(NIPAAm-*co*-AMPS) gels crosslinked by complex **6**, which follow the redox swelling trend typical for the conventional BZ gels, was observed, at room temperature, for the gel having 30 mol% of AMPS (**Figure 5**). To achieve the highest swelling/contraction contrast in this regime, all the following experiments were therefore performed using redox-active Ru crosslinker **6** and poly(NIPAAm-*co*-AMPS, 30 mol%) gel formulation.

The prepolymer solution was deposited onto a micropost array (diameter: 10 μm, height: 100 μm, pitch: 25 μm), allowed to cure under a confining glass slide surface and, after purification from unreacted starting materials (see the Experimental Section for details), was immersed into a BZ reaction solution (900×10^{-3} M HNO_3, 168×10^{-3} M $NaBrO_3$, 63×10^{-3} M malonic acid). After ≈45 min induction period, a sustained oscillation pattern of color changes propagating though the gel area was clearly observed (Movies S1 and S2 in the Supporting Information). In the presence of sufficient amounts of BZ reagents, the oscillations continued undisturbed for ≈9 h, after which time the observations were stopped. These experiments clearly demonstrated that the poly(NIPAAm-*co*-AMPS) gels crosslinked by the new type of the redox-active crosslinker, **6**, actively support BZ reaction for prolonged time and that ester linkages of the ligand **4** are sufficiently stable within the crosslinked gel network to withstand the highly acidic aqueous medium of BZ reaction. The oscillatory behavior of the gel was quantified using image analysis (**Figure 6**).

Over ≈10 min, a line positioned diagonally to the frame and approximately normally to the direction of the propagation of the front of the chemical wave was imaged under an optical microscope every 1 s and the acquired images were stacked on top of each other. The analysis of the resulting composite image showed that the period of chemical oscillations was ≈50 s and the chemical wave propagated through the gel at a linear velocity of ≈50 μm s^{-1}. Though direct comparison of the oscillation periods for different gel systems

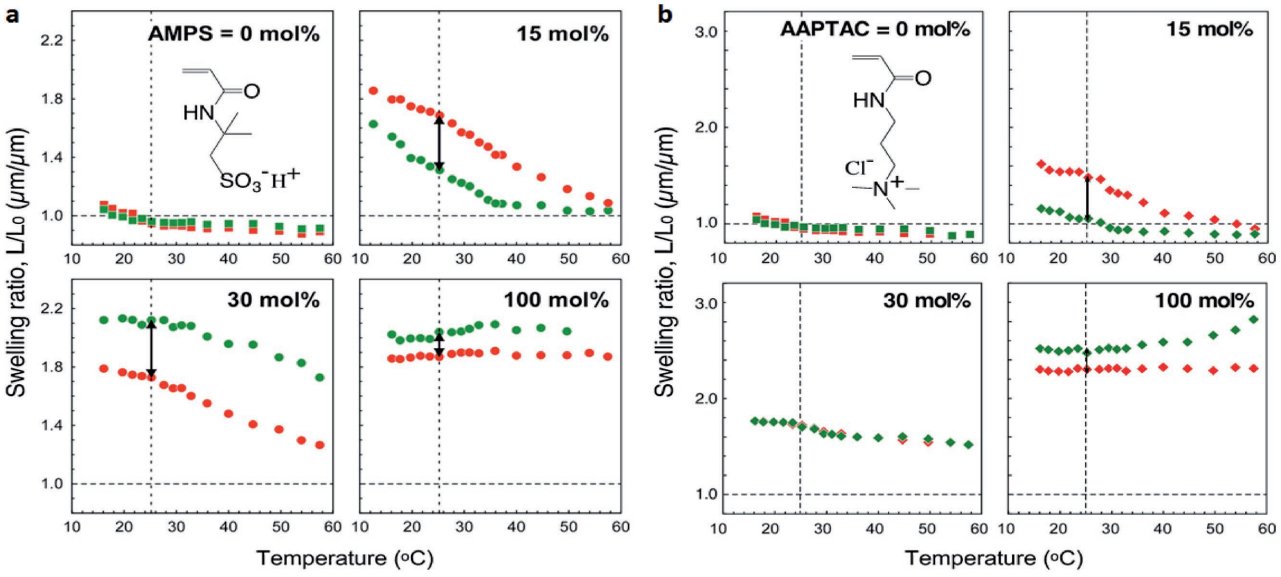

Figure 4. Temperature dependence of swelling ratios of PNIPAAm gels having different amounts of hydrophilic comonomers crosslinked by complex **6**. a) poly(NIPAAm-*co*-AMPS) gels with different amounts of AMPS. b) poly(NIPAAm-*co*-AAPTAC) gels with different amounts of AAPTAC. Oxidized states shown in green were achieved by immersing the gels in the solution of 900×10^{-3} M HNO_3, 168×10^{-3} M $NaBrO_3$. Reduced states shown in red were achieved by immersing the gels in the solution of 900×10^{-3} M HNO_3, 168×10^{-3} M $NaNO_3$. The amount of crosslinker **6** charged to the prepolymer mixture is kept at 1 mol% for all samples. The swelling ratios were calculated from measuring the distances between the centers of the holes, L and L_0 as described in Figure 3.

is not straightforward, we believe that the ≈50 s period of oscillations we measured in our system is among the faster ones compared to those found by other groups, both in conventional gels and in the gels crosslinked by other Ru complexes.[13a–c,f,14b]

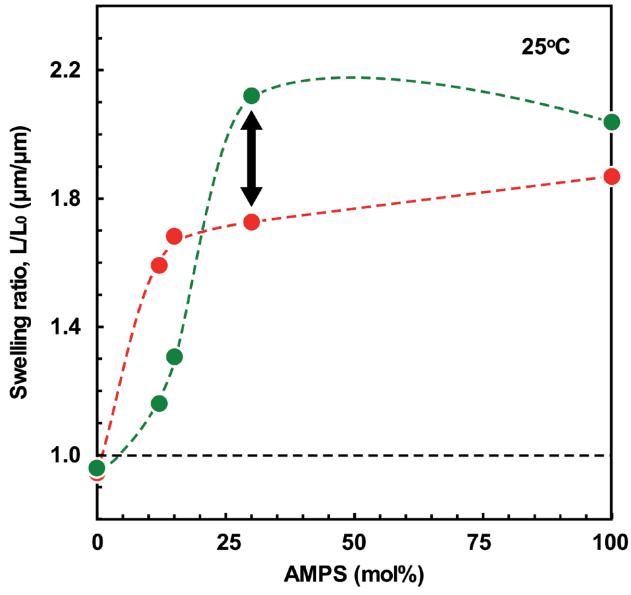

Figure 5. Swelling ratio contrast between the reduced (red) and oxidized (green) forms of poly(NIPAAm-*co*-AMPS) gels as a function of AMPS loading at room temperature. The swelling ratios were calculated from measuring the distances between the centers of the holes, L and L_0 as described in Figure 3.

2.2.4. Volume Oscillations of a Free-Standing Functional Gel

To probe the capacity of the prepared gel to undergo volume self-oscillations, without being restricted by rigid skeletal elements of micropost array, we prepared a free-standing sample of the poly(NIPAAm-*co*-AMPS, 30 mol%) crosslinked by **6** and immersed it in a BZ reaction mixture, using the procedure shown in Figure 3. The presence of the regular array of holes enabled very precise analysis of the mechanical deformations in the gel. The chemical wave passing through the gel volume did, indeed, exhibit periodic mechanical contractions and expansions demonstrating effective chemomechanical coupling, as was anticipated (Movie S3, Supporting Information). Quantification of the observed volume oscillation produced the following parameters: period of ≈80 s and propagation velocity of ≈85 μm s^{-1} (**Figure 7**). The volume self-oscillation was analyzed in two more directions and showed similar results (Figure S2, Supporting Information), additionally confirming the quantification presented in Figure 7. Remarkably, even the gel composition having 15% of AMPS comonomer, which is exhibiting reverse swelling/contraction relationship–expanded, when reduced, and contracted, when oxidized—can be utilized as well in designing active self-oscillating BZ gels, as Figure S3 of the Supporting Information demonstrates. The magnitude of the volume oscillations is not very high, especially when compared to those reported for pH-responsive hydrogels, but it nevertheless suggests that **6**-crosslinked poly(NIPAAm-*co*-AMPS) can be incorporated into a variety of functional materials where conventional poly(NIPAAm-*co*-Ru(Bpy)$_2$(4-Me, 4′-Vi-Bpy)) gels have been utilized to provide self-sustained oscillations and autonomic chemomechanical action unattainable in regular pH-responsive gels.

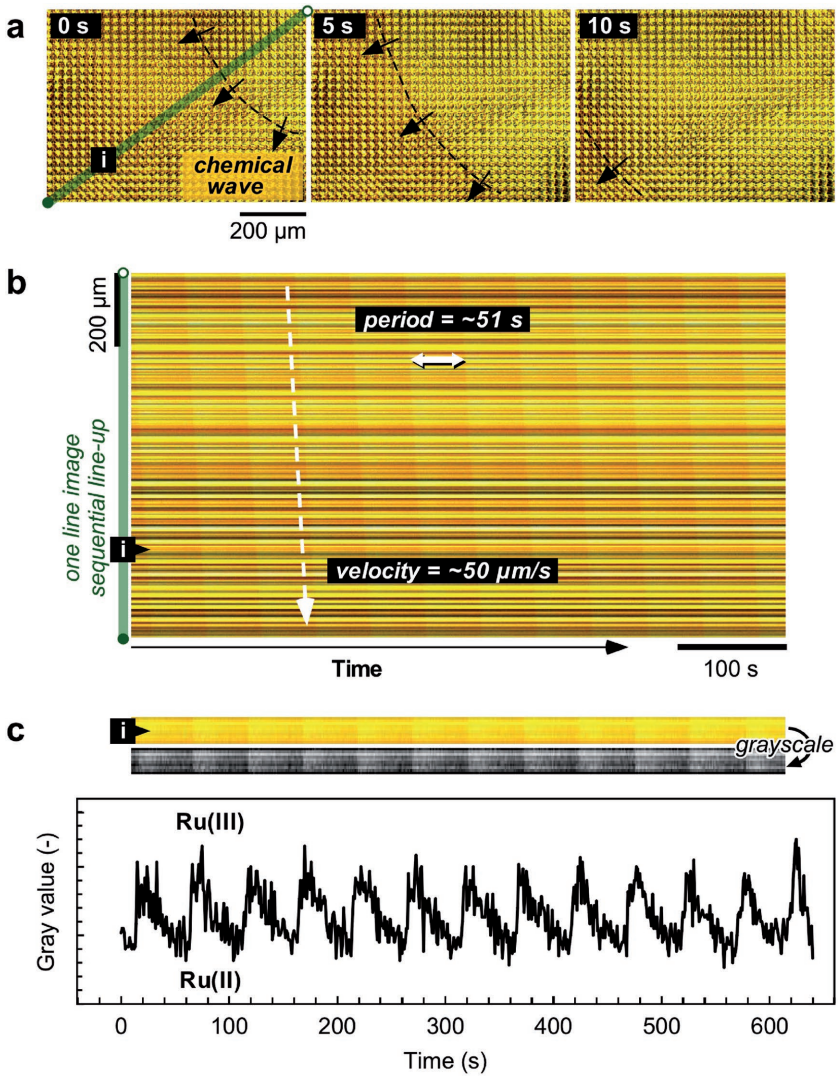

Figure 6. Quantification of gel oscillations and chemical wave propagation of a gel formed on a microstructure array. The quantification is based on the analysis of Movie S1 (Supporting Information). a) Still frames from Movie S1 (Supporting Information) showing the direction of propagation of chemical wave and the straight line (green) chosen for image analysis. b) Stacked images of the selected line taken every 1 s showing periodicity and speed of the chemical wave. c) Oscillation curve derived from (b) by analyzing the evolution of the gray value over a period of ≈10 min.

3. Conclusion

A library of synthesized and carefully characterized polymerizable bipyridine and biquinoline ligands and their representative Ru(II) and Fe(II) complexes are shown to offer a variety of hybrid polymer architectures, in which metal complexes serve as crosslinkers. These redox-active crosslinkers are demonstrated to have reduction potentials compatible with those needed for triggering self-oscillating BZ reaction and several examples of these reactions triggered by one representative of this new family of gels are shown. Importantly, we have observed and are reporting a previously unknown swelling behavior of ruthenium complex-crosslinked redox-active functional PNIPAAm hydrogels that exhibit a switch in the order of swelling ratios of the gels in reduced and oxidized forms, depending on the molar percentage of a hydrophilic comonomer—AMPS or AAPTAC. Differing from the typical poly(NIPAAm-*co*-Ru(bpy)$_3$) gels prepared with methylenebisacrylamide,[13,15] this unprecedented behavior indicates that a simple charge-based and respective hydration-based swelling/deswelling model is not operational in the gels of this type, and the mechanism is likely to involve comonomer concentration-dependent conformational rearrangement of the poly(NIPAAm-*co*-AMPS) and poly(NIPAAm-*co*-AAPTAC) gel networks, leading to the opposite trends in their overall hydrophilicity. We believe that these examples open a door toward higher modularity in the field of BZ-active metallopolymers. With a broad library of ligands and metal centers (not restricted to Ru and Fe only), a wide variety of polymer types and architectures will be available, offering significant advances in the field of chemomechanically active functional materials and their applications in responsive and self-regulated systems.

4. Experimental Section

General: Most materials and solvents were purchased from Aldrich and used as received, without further purification, except where specified otherwise. Syntheses of metal complexes were performed in a Braun nitrogen-filled drybox using commercial dry solvents, while syntheses of the ligands were performed using standard experimental techniques under nitrogen atmosphere when necessary. Elemental analyses were performed by Micro-Analysis, Inc., Wilmington, DE. Cyclic voltammetry data were obtained from KB-Analytical, Oakdale, CT. HR electrospray ionization (ESI)-time-of-flight (TOF) MS data of synthesized ligands were obtained using Agilent 6210 ESI-time-of-flight liquid chromatography (LC)–MS, in acetonitrile as a solvent, at Small Molecule Mass Spectrometry Facility of Harvard FAS-Center for Systems Biology. As necessary, the reaction progress was followed using high-performance (HP)LC (Agilent 1200, C18 column, acetonitrile–water/5% formic acid mobile phase, UV detection at 254 nm). Sodium [2,2′-bipyridine]-4,4′-dicarboxylate[8] (**2**), [2,2′-bipyridine]-4,4′-dicarbonyl dichloride (**3**)[42,43] were synthesized using literature procedures. The epoxy microstructure arrays were prepared from Si masters by double replication, as described previously, either with glycidylmethacrylate comonomer (GMA; epoxy UVO-114:GMA = 9:1) when attachment of the gels to microstructures was intended or without it when a free-standing gel was to be peeled off from the Au/Pd coated arrays.

HRMS of Metal Complexes: The samples were dissolved in dichloromethane and introduced into the electrospray source of a Bruker Maxis Impact, high-resolution time-of-flight mass spectrometer. The resolving power ($m/\Delta m$) obtained on the ions was between 20 000 and 40 000. The instrument was calibrated with Agilent ESI-TOF tune mix in the range of interest prior to analysis of the sample and this external calibration was used for all samples analyzed. Relative errors

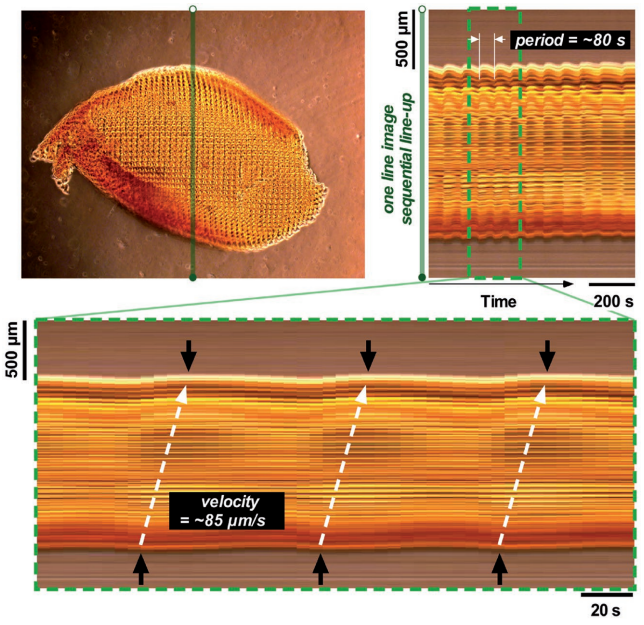

Figure 7. Quantification of gel oscillations and chemical wave propagation in the free-standing gel sample bearing a regular array of holes. The quantification is based on the analysis of Movie S3 (Supporting Information) with images taken every 5 s. The gel used was poly(NIPAAm-*co*-AMPS crosslinked by **6** at 30% AMPS loading.

obtained on all samples were <5 ppm. Samples were introduced using direct infusion at 3 µL min^{-1} with a syringe pump. Dichloromethane was selected due to its ability to keep the samples dry during analysis.

FTIR: The spectra of neat powder materials were acquired using Bruker Vertex-70 spectrometer equipped with a PIKE attenuated total reflectance (ATR) accessory with a ZnSe crystal.

NMR: NMR spectra were acquired using either Varian Mercury 300 MHz or Varian Unity/Inova 500 MHz or Varian Mercury 400 MHz spectrometers at ambient temperatures. The ^{1}H and $^{13}C\{^{1}H\}$ spectra were referenced against signals of TMS as an internal or external standard and $^{19}F\{^{1}H\}$ spectra to $CFCl_3$ as an external standard. The NMR solvents $(CD_3)_2SO$, $CDCl_3$, C_6D_6, CD_3NO_2, $(CD_3)_2CO$ were used as received, without further purification.

Cyclic Voltammetry: The cyclic voltammograms were measured using Digi-Ivy DY 2100 potentiostat under argon atmosphere in 0.10 M tetrabutylammonium perchlorate in acetonitrile as electrolyte, with Ag/0.01 M $AgNO_3$ in acetonitrile as reference electrode, 3 mm glassy carbon as working electrode, and platinum wire as counter electrode. Based on ferrocene/ferricinium standard run under the same conditions as the samples, appropriate factors were introduced to obtain corresponding values of redox potentials referenced against SCE and SHE.[38]

*Synthesis of Bis(4-Vinylbenzyl) [2,2′-Bipyridine]-4,4′-Dicarboxylate (**4**)*: Benzylic nucleophilic substitution of chloride by sodium carboxylate installed on bipyridine core is not fast, but works very smoothly at a slightly elevated temperature in dimethylsulfoxide (DMSO) as a solvent, in the dark, to prevent polymerization of 1-(chloromethyl)-4-vinylbenzene,[44] yielding the desired diester (**4**) in one step as a fine crystalline white powder (Scheme 1a). To 1.0 g (3.22 mmol, 92.7% pure) of sodium [2,2′-bipyridine]-4,4′-dicarboxylate (**2**) slurried in 40 mL DMSO was added at room temperature under N_2 blanket 1.034 µL (1.120 g, 6.60 mmol, 90% pure, 2.05 eq.) of 1-(chloromethyl)-4-vinylbenzene. The mixture was stirred at 40 °C in the dark for 26 h and then for additional 68 h at room temperature, after which it was quenched upon cooling with 60 mL of DI water. The resulting slurry was filtered at 12 °C and the crude solid product was washed on the filter with 2 × 10 mL of water followed by 2 × 4 mL of dichloromethane (DCM)/hexane (5:95, v/v). After drying, the solid was additionally purified (from the mono-substituted impurity) by reslurrying it in hot methanol, and subsequent drying under high vacuum till constant weight. Yield: 1.116 g (72.8%) of white powder. ^{1}H-NMR (300 MHz, DMSO-d_6, δ): 8.95 (d, J = 5.4 Hz, 2H), 8.85(s, 2H), 7.98 (m, 2H), 7.52 (m, 8H), 6.76 (dd, J_1 = 10.7 Hz, J_2 = 17.6 Hz, 2H), 5.88 (d, J = 18.1 Hz, 2H), 5.43 (s, 4H), 5.17 (d, J = 10.7 Hz, 2H). $^{13}C\{^{1}H\}$-NMR (DMSO-d_6, 125 MHz, δ): 164.38, 155.42, 150.93, 138.31, 137.28, 136.18, 135.09, 128.76, 126.36, 123.49, 119.25, 114.90, 66.97. FTIR-ATR (powder, ν, cm^{-1}): 1720 (C=O). Elemental Analysis: calcd for $C_{30}H_{24}N_2O_4$ (476.52): C 75.61, H 5.08, N 5.88; found: C 73.86, H 4.82, N 6.05. HRMS (ESI-TOF, m/z): 477.18233 (MH^+) versus 477.18088 (theory). Single crystals suitable for an X-ray crystallographic study were grown over several days by a slow vapor diffusion of pentane into a toluene solution of pure **4** at −35 °C.

*Synthesis of [2,2′-Bipyridine]-4,4′-Dicarbonyl Dichloride (**3**)*: [2,2′-bipyridine]-4,4′-dicarboxylic acid (**1**, Alfa Aesar, 0.500 g, 2.047 mmol) was combined in a 50 mL round-bottom flask with thionyl chloride (8 mL, 110 mmol, 53.5 eq.) and refluxed under nitrogen blanket for 24 h. The mixture was allowed to cool to room temperature, after which the volatiles were removed under high vacuum to yield the desired product as a yellow solid that was subsequently used in preparation of **5** without further purification.[42,43,45]

*Synthesis of N4,N4′-Bis(4-Vinylphenyl)-2,2′-Bipyridine-4,4′-Dicarboxamide (**5**)*: To a precooled to 0°C solution of [2,2′-bipyridine]-4,4′-dicarbonyl dichloride (**3**) (0.575 g, 2.047 mmol) in 10 mL of tetrahydrofuran (THF) was added dropwise (over 8 min) a solution of 4-vinylaniline (0.860 g, 7.2 mmol, 3.52 eq.) and triethylamine (0.829 g, 8.19 mmol, 4.0 eq.) in 10 mL THF upon vigorous stirring under N_2 blanket. After 40 min, the cooling was removed and the formed slurry was allowed to warm to room temperature. Upon warming, the slurry was diluted with 5 mL THF and allowed to react for an additional 20 h. The precipitated solid was isolated by filtration and washed successively with 10, 7.5, and 7.5 mL of fresh THF followed with 2 × 5 mL of 3% ammonia solution and 6 × 10 mL deionized (DI) water. Drying under high vacuum till constant weight yielded the desired product as a white fluffy powder.[46] Yield: 0.800 g (88%). ^{1}H-NMR (300 MHz, DMSO-d_6, δ): 10.79 (s, 2H), 8.97 (d, J = 4.9 Hz, 2H), 8.92 (s, 2H), 8.00 (dd, J_1 = 1.5 Hz, J_2 = 4.9 Hz, 2H), 7.83 (d, J = 8.8 Hz, 4H), 7.52 (d, J = 8.8 Hz, 4H), 6.73 (dd, J_1 = 10.7 Hz, J_2 = 17.6 Hz, 2H), 5.81 (d, J = 18.1 Hz, 2H), 5.24 (d, J = 10.7 Hz, 2H). $^{13}C\{^{1}H\}$-NMR (125 MHz, DMSO-d_6, δ): 163.88, 155.47, 150.20, 143.38, 138.32, 136.11, 133.14, 126.54, 122.39, 120.53, 118.58, 113.36. FTIR-ATR (powder, ν, cm^{-1}): 1649 (C=O), 3285 (N−H). Due to poor solubility, no additional purification was attempted. HRMS (ESI-TOF, m/z): 447.18253 (MH^+), 469.16436 ($M + Na^+$) versus 447.18155, 469.16350 (theory).

*Synthesis of [(bpy)$_2$Ru(**4**)](PF$_6$)$_2$ (**6**)*: (a) In a glovebox, commercial-grade cis$(bpy)_2RuCl_2$ hydrate (4.9% H_2O, 200 mg, 0.393 mmol, Aldrich) was dissolved in 6 mL of methanol and to the resulting dark purple solution was added $AgPF_6$ (100 mg, 0.395 mmol). The mixture was stirred in the dark for 18.5 h, after which the deep red solution was filtered to remove the formed AgCl. The solvent was removed under vacuum and the residue formed was additionally triturated with 4 mL pentane, and dried high vacuum till constant weight to yield 300 mg (99.6%) of deep red microcrystalline solid, assumed to be $[(bpy)_2Ru(CH_3OH)_2](PF_6)_2$,[37] which was used without further purification in the next step. (b) To $[(bpy)_2Ru(CH_3OH)_2](PF_6)_2$ obtained in (a) (102 mg, 0.133 mmol) dissolved in 5 mL of acetone was added **4** (62 mg, 0.130 mmol) and the mixture was stirred at room temperature for 26 h. The solvent was removed under vacuum and the resulting dark red residue was reprecipitated from 2 mL of dichloromethane by the addition of 4 mL of pentane. The formed dark red solid was filtered and dried under vacuum to yield the desired product as a brick-red microcrystalline solid. Yield: 0.153 g (99.8%). ^{1}H-NMR (500 MHz, DMSO-d_6, δ): 9.34 (br s, 2H), 8.85 (t, J = 8.3 Hz, 4H), 8.19 (symm m, 4H), 7.97 (2nd order d, J = 5.9 Hz, 2H), 7.92 (2nd order dd, J_1 = 1.5 Hz, J_2 = 5.9 Hz, 2H), 7.74 (d, J = 5.4 Hz, 2H), 7.69 (d, J = 5.4 Hz, 2H), 7.55 (symm pseudo dt, J_d = 0.98 Hz, J_t = 6.3 Hz, 2H), 7.51–7.46 (overlapping m, 10H), 6.75 (dd, J_1 = 11.2 Hz, J_2 = 17.6 Hz, 2H), 5.86 (d, J = 17.6 Hz, 2H), 5.45 (symm 2nd order m, 4H), 5.29 (d, J = 11.2 Hz). $^{13}C\{^{1}H\}$-NMR (125 MHz, DMSO-d_6, δ): 163.32, 157.35, 156.24, 156.17, 152.44, 151.63,

151.02, 138.39 (br) 137.53, 137.27, 136.11, 134.94, 128.61, 128.06, 127.96, 126.79, 126.22, 124.58, 123.95, 114.91, 67.25. $^{19}F\{^1H\}$-NMR (282 MHz, DMSO-d_6, δ), −70.5 (d, J = 711 Hz, PF_6). FTIR-ATR (powder, ν, cm^{-1}): 1719 (C=O). Elemental Analysis: calcd for $C_{50}H_{40}F_{12}N_6O_4P_2Ru$ (1179.89): C 50.90, H 3.42, N 7.12; found (average of 3): C 49.56, H 3.48, N 7.38. HRMS (ESI-TOF, m/z): 1035.1792 ($[M\text{-}(PF_6)]^+$) versus 1035.1796 (theory for $C_{50}H_{40}F_6N_6O_4PRu$), 445.1068 ($[M\text{-}2(PF_6)]^{2+}$) versus 445.1079 (theory for $C_{50}H_{40}N_6O_4Ru$, 890.2155) with the expected isotope patterns. Deep red-brown needle-shaped single crystals of **6**·0.67 CH_2Cl_2 suitable for an X-ray crystallographic study were grown by slow vapor diffusion of pentane into a dichloromethane solution of pure **6** at room temperature over several days.

*Synthesis of [(bpy)$_2$Ru(**5**)](PF$_6$)$_2$ (**7**)*: Obtained as described before $[(bpy)_2Ru(CH_3OH)_2](PF_6)_2$ (100 mg, 0.130 mmol) and **5** (62 mg, 0.130 mmol) were combined in 8 mL acetone to form a slurry. The reaction vessel was sealed and the mixture was stirred at slow reflux in an aluminum heating block at 65–70 °C for 46 h. The mixture was filtered, the filtrate was concentrated under vacuum and the resulting dark red residue was triturated with 3 mL of pentane and, after removal of pentane, reprecipitated from 3 mL of dichloromethane by the addition of 6 mL of pentane. The solid was collected by filtration, additionally reslurried in 3 mL of pentane and dried under vacuum to provide the desired product as a red powder. Yield: 0.144 g (96.3%). ^{1}H-NMR (300 MHz, DMSO-d_6, δ): 10.84 (br s, 2H), 9.37 (br s, 2H), 8.88 (d, J = 8.3 Hz, 4H), 8.22 (m, 4H), 7.98 (m, 4H), 7.81–7.75 (overlapping m, 8H), 7.60–7.51 (overlapping m, 8H), 6.72 (dd, J_1 = 11.2 Hz, J_2 = 18.0 Hz, 2H), 5.80 (d, J = 17.6 Hz, 2H), 5.24 (d, J = 11.2 Hz, 2H). $^{13}C\{^1H\}$-NMR (125 MHz, DMSO-d_6, δ): 162.40, 156.97 (br) 156.47, 156.32, 151.99, 151.42, 151.19, 142.82, 138.36, 138.34, 137.86, 136.01, 133.57, 128.09, 128.01, 126.71, 125.94, 124.61, 122.59, 120.57, 113.68. FTIR-ATR (powder, ν, cm^{-1}): 1676 (C=O). Elemental Analysis: calcd for $C_{48}H_{38}F_{12}N_8O_2P_2Ru$ (1149.86): C 50.14, H 3.33, N 9.74; found (average of 3): C 48.89, H 3.37, N 9.62. HRMS (ESI-TOF, m/z): 1005.1855 ($[M\text{-}(PF_6)]^+$) versus 1005.1803 (theory for $C_{48}H_{38}F_6N_6O_4PRu$), 430.1105 ($[M\text{-}2(PF_6)]^{2+}$) versus 430.1081 (theory for $C_{48}H_{38}N_8O_2Ru$, 860.2161) with the expected isotope patterns.

*Synthesis of [Fe(**4**)$_3$](BF$_4$)$_2$ (**8**)*: In order to sufficiently solubilize the starting complex and the ligands, a highly polar aprotic nitromethane solvent was chosen[47] (or its mixture with dichloromethane). $Fe(H_2O)_6(BF_4)_2$ (34 mg, 0.101 mmol) and **4** (145 mg, 0.305 mmol) were combined in 5 mL of nitromethane. The mixture immediately turned dark purple. The reaction was allowed to proceed at room temperature for 22 h. The solvent was removed under vacuum, the resulting oily residue was redissolved in 3 mL of dichloromethane and dried under vacuum. The crude product was isolated by precipitation from its solution in 3 mL dichloromethane upon addition of 4.5 mL pentane in a drybox freezer at −35 °C. Drying of the dark purple solid under high vacuum produced desired **8** as dark purple glassy flakes. Yield: 0.165 g (98.5%). ^{1}H-NMR (500 MHz, CD_3NO_2, δ): 9.13 (s, 6H), 7.90 (d, J = 4.6 Hz, 6H), 7.73 (d, J = 5.0 Hz, 6H), 7.49 (m, 24H), 6.79 (dd, J_1 = 11.0 Hz, J_2 = 17.4 Hz, 6H), 5.85 (d, J = 17.4 Hz, 6H), 5.45 (s, 12H), 5.32 (d, 11.0 Hz, 6H). $^{13}C\{^1H\}$-NMR (125 MHz, CD_3NO_2, δ): 164.91, 161.04, 156.69, 141.91, 139.61, 137.67, 136.44, 130.31, 127.87, 127.78, 124.76, 115.62, 69.35. $^{19}F\{^1H\}$-NMR (282 MHz, $CDCl_3$, δ), −151.01 (BF_4). FTIR-ATR (powder, ν, cm^{-1}): 1726 (C=O). Elemental analysis: calcd for $C_{90}H_{72}B_2F_8FeN_6O_{12}$ (1659.02): C 65.16, H 4.37, N 5.07; found (average of 3): C 63.43, H 4.25, N 5.23. HRMS (ESI-TOF, m/z): 742.2287 ($[M\text{-}2(BF_4)]^{2+}$) versus 742.2275 (theory for $C_{90}H_{72}FeN_6O_{12}$, 1484.4558) with the expected isotope pattern.

*Synthesis of [Fe(**5**)$_3$](BF$_4$)$_2$ (**9**)*: $Fe(H_2O)_6(BF_4)_2$ (34 mg, 0.101 mmol) and **5** (136 mg, 0.305 mmol) were combined in 10 mL of 1:1 (v/v) solution of dichloromethane and nitromethane. The mixture acquired a pink tint. The reaction was allowed to proceed at room temperature for 22 h, after which time the solvents were removed under vacuum. Drying of the resulting dark purple solid under high vacuum produced desired **9** as a dark purple powder. Yield: 0.158 g (100%). ^{1}H-NMR (500 MHz, CD_3NO_2, δ): 9.15 (br s, 6H), 9.04 (br s, 6H), 7.95–7.90 (m, 12H), 7.75 (d, J = 8.2 Hz, 12H), 7.53 (d, J = 8.2 Hz, 12H), 6.77 (dd, J_1 = 11.0 Hz, J_2 = 17.4 Hz, 6H), 5.81 (d, J = 17.9 Hz, 6H), 5.27 (d, J = 11.0 Hz, 6H). $^{13}C\{^1H\}$-NMR (125 MHz, CD_3NO_2, δ): 163.73, 161.11, 156.63, 146.53, 138.80, 137.49, 136.26, 128.22, 126.71, 123.16, 122.05, 114.56. FTIR-ATR (powder, ν, cm^{-1}): 1678, 1653 (C=O), 3295 (N−H). Elemental analysis: calcd for $C_{84}H_{66}B_2F_8FeN_{12}O_6$ (1568.95): C 64.30, H 4.24, N 10.71; found (average of 3): C 63.36, H 4.32, N 10.63. HRMS (ESI-TOF, m/z): 1481.4622 ($[M\text{-}(BF_4)]^+$) versus 1481.4607 (theory for $C_{84}H_{66}BF_4FeN_{12}O_6$) with the expected isotope pattern.

X-Ray Crystallography: A crystal was mounted on a diffractometer and the data were collected at 100 K. The intensities of the reflections were collected by means of a Bruker APEX II DUO CCD diffractometer (Cu Kα radiation, λ = 1.54178 Å), and equipped with an Oxford Cryosystems nitrogen flow apparatus. The collection method involved 1.0° scans in ϖ at 30°, 55°, 80°, and 115° in 2θ. Data integration down to 0.84 Å resolution was carried out using SAINT V7.46 A (Bruker diffractometer, 2009) with reflection spot size optimization. Absorption corrections were made with the program SADABS (Bruker diffractometer, 2009). The structures were solved by the direct methods procedure and refined by least-squares methods against F^2 using SHELXS-97 and SHELXL-97[48] with OLEX 2 interface.[49] Nonhydrogen atoms were refined anisotropically, and hydrogen atoms were allowed to ride on the respective atoms. The ORTEP plots were produced with SHELXL-97 program.

*Preparation of Hydrogels Based on Complexes **6** and **8***: A DMSO solution containing NIPAAm, Ru (1 mol%) or Fe (1 mol%) metal complex crosslinker, radical initiator Darocur 1173 (2-hydroxy-2-methyl-1-phenyl-1-propanone, 2–5 wt% with regard to NIPAAm) was deposited onto a plasma-treated micropost array substrate, covered with a glass slide and allowed to cure under UV irradiation. The UV irradiation parameters were as follows: ≈10 mW cm^{-2} at 365 nm, 6–10 min, distance between lamp and sample ≈20–25 cm. After curing, the samples were immersed sequentially in DMSO for 3 h, to peel off the cover slip and remove the unreacted metal complex crosslinker, and in 10×10^{-3} M HNO_3 for 1 d (for the gels attached to the microstructures) or in DI water (for the experiments where gels were to be peeled off from Au/Pd coated substrates), to finally condition them to the experiments that followed. Following these treatments, the clean transparent gels were immersed into the appropriate solutions for swelling ratio measurements (900×10^{-3} M HNO_3, 168×10^{-3} M $NaNO_3$ or 900×10^{-3} M HNO_3, 168×10^{-3} M $NaBrO_3$) or into a BZ reaction mixture (900×10^{-3} M HNO_3, 168×10^{-3} M $NaBrO_3$, 63×10^{-3} M malonic acid) for the BZ experiments on a substrate or as a peeled-off free-standing sample. The poly(NIPAAm-*co*-AMPS) and poly(NIPAAm-*co*-AAPTAC) gels containing 15%, 30%, or 100% of the AMPS or AAPTAC hydrophilic comonomers were prepared in full analogy, except the charges of the monomers into the prepolymer mixture were adjusted accordingly. The prepolymer compositions used are shown in the Supporting Information.

Image Analyses: The images were analyzed using software ImageJ. After converting color images to gray scale, the gray scale level was analyzed to produce oscillation curve in Figure 6, with images taken every 1 s. Spatiotemporal diagram in Figure 7 was obtained by taking one line image sequential line-up. The interval between taking images was 5 s.

[CCDC ##1559096-1559097 contains the supplementary crystallographic data for this paper. These data can be obtained free of charge from The Cambridge Crystallographic Data Centre via www.ccdc.cam.ac.uk/data_request/cif.]

Supporting Information

Supporting Information is available from the Wiley Online Library or from the author.

Acknowledgements

The work was supported by the DOE under Award DE-SC0005247. K.O. is thankful for JSPS Research Fellowship and JSPS Postdoctoral Fellowship

for Research Abroad. The authors thank Dr. Sunia A. Trauger (Harvard FAS Center for Systems Biology, Small Molecule Mass Spectrometry) for HRMS data of metal complexes, Dr. Shao-Liang Zheng (Harvard Department of Chemistry and Chemical Biology, X-Ray Laboratory) for his help with the X-ray data collection and structure determination, Chris Johnson, and Jack Alvarenga for technical assistance.

Conflict of Interest

The authors declare no conflict of interest.

Keywords

catalysis, hybrid materials, hydrogels, stimuli-responsive materials

Received: July 25, 2017
Revised: August 21, 2017
Published online:

[1] V. Balzani, A. Juris, M. Venturi, S. Campagna, S. Serroni, *Chem. Rev.* **1996**, *96*, 759.
[2] A. Juris, V. Balzani, F. Barigelletti, S. Campagna, P. Belser, A. Vonzelewsky, *Coord. Chem. Rev.* **1988**, *84*, 85.
[3] D. G. H. Hetterscheid, J. N. H. Reek, *Angew. Chem., Int. Ed.* **2012**, *51*, 9740.
[4] R. D. Costa, E. Orti, H. J. Bolink, F. Monti, G. Accorsi, N. Armaroli, *Angew. Chem., Int. Ed.* **2012**, *51*, 8178.
[5] D. A. Nicewicz, D. W. C. MacMillan, *Science* **2008**, *322*, 77.
[6] B. S. Howerton, D. K. Heidary, E. C. Glazer, *J. Am. Chem. Soc.* **2012**, *134*, 8324.
[7] V. Aranyos, J. Hjelm, A. Hagfeldt, H. Grennberg, *Dalton Trans.* **2003**, *7*, 1280.
[8] P. G. Hoertz, A. Staniszewski, A. Marton, G. T. Higgins, C. D. Incarvito, A. L. Rheingold, G. J. Meyer, *J. Am. Chem. Soc.* **2006**, *128*, 8234.
[9] a) I. Manners, *Synthetic Metal-Containing Polymers*, Wiley-VCH Verlag GmbH & Co. KGaA, Weinheim **2004**, p. 203; b) G. R. Whittell, M. D. Hager, U. S. Schubert, I. Manners, *Nat. Mater.* **2011**, *10*, 176.
[10] a) I. Rubinstein, A. J. Bard, *J. Am. Chem. Soc.* **1980**, *102*, 6641; b) C. D. Clark, J. D. Debad, E. H. Yonemoto, T. E. Mallouk, A. J. Bard, *J. Am. Chem. Soc.* **1997**, *119*, 10525.
[11] a) C. M. Elliott, F. Pichot, C. J. Bloom, L. S. Rider, *J. Am. Chem. Soc.* **1998**, *120*, 6781; b) G. de Ruiter, M. Lahav, M. E. van der Boom. *Acc. Chem. Res.* **2014**, *47*, 3407; c) N. E. Dov, S. Shankar, D. Cohen, T. Bendikov, K. Rechav, L. J. W. Shimon, M. Lahav, M. E. van der Boom, *J. Am. Chem. Soc.* **2017**, *139*, 11471.
[12] S. J. Payne, G. L. Fiore, C. L. Fraser, J. N. Demas, *Anal. Chem.* **2010**, *82*, 917.
[13] a) R. Yoshida, T. Takahashi, T. Yamaguchi, H. Ichijo, *J. Am. Chem. Soc.* **1996**, *118*, 5134; b) R. Yoshida, *Adv. Mater.* **2010**, *22*, 3463; c) Y. Hara, R. Yoshida, *Langmuir* **2005**, *21*, 9773; d) Y. Hara, R. Yoshida, *Macromol. Rapid Commun.* **2009**, *30*:1656; e) Y. Hara, T. Sakai, S. Maeda, S. Hashimoto, R. Yoshida, *J. Phys. Chem. B* **2005**, *109*, 23316; f) Y. Hara, R. Yoshida, *J. Phys. Chem. B* **2005**, *109*, 9451; g) R. Yoshida, T. Sakai, S. Ito, T. Yamaguchi, *J. Am. Chem. Soc.* **2002**, *124*, 8095.
[14] a) Y. Zhang, N. Li, J. Delgado, N. Zhou, R. Yoshida, S. Fraden, I. R. Epstein, B. Xu, *Soft Matter* **2012**, *8*, 7056; b) Y. Zhang, N. Zhou, S. Akella, Y. Kuang, D. Kim, A. Schwartz, M. Bezpalko, B. M. Foxman, S. Fraden, I. R. Epstein, B. Xu, *Angew. Chem., Int. Ed.* **2013**, *52*, 11494.
[15] a) Y. Hara, K. Fujimoto, H. Mayama, *J. Phys. Chem. B* **2014**, *118*, 608; b) Y. Hara, H. Mayama, Y. Yamaguchi, K. Fujimoto, *Chem. Lett.* **2014**, *43*, 673.
[16] I. Y. Konotop, I. R. Nasimova, N. G. Rambidi, A. R. Khokhlov, *Polym. Sci., Ser. B* **2009**, *51*, 383.
[17] R. Yerushalmi, A. Scherz, M. E. van der Boom, H.-B. Kraatz, *J. Mater. Chem.* **2005**, *15*, 4480.
[18] B. P. Belousov, *Compil. Abstr. Radiat. Med.* **1959**, *147*, 1.
[19] A. M. Zhabotinskii, *Biophysics* **1964**, *9*, 329.
[20] P. Yuan, O. Kuksenok, D. E. Gross, A. C. Balazs, J. S. Moore, R. G. Nuzzo, *Soft Matter* **2013**, *9*, 1231.
[21] H. Zhou, Z. Zheng, Q. Wang, G. Xu, J. Li, X. Ding, *RSC Adv.* **2015**, *5*, 13555.
[22] P. K. Ghosh, T. G. Spiro, *J. Am. Chem. Soc.* **1980**, *102*, 5543.
[23] H. D. Abruna, A. I. Breikss, D. B. Collum, *Inorg. Chem.* **1985**, *24*, 987.
[24] J. Kaschig, D. Lohmann, *US4424359 A*, **1984**.
[25] A. Sidorenko, T. Krupenkin, A. Taylor, P. Fratzl, J. Aizenberg, *Science* **2007**, *315*, 487.
[26] P. Kim, L. D. Zarzar, X. M. He, A. Grinthal, J. Aizenberg, *Curr. Opin. Solid State Mater. Sci.* **2011**, *15*, 236.
[27] L. D. Zarzar, J. Aizenberg, *Acc. Chem. Res.* **2014**, *47*, 530.
[28] A. Sidorenko, T. Krupenkin, J. Aizenberg, *J. Mater. Chem.* **2008**, *18*, 3841.
[29] L. D. Zarzar, P. Kim, J. Aizenberg, *Adv. Mater.* **2011**, *23*, 1442.
[30] X. He, M. Aizenberg, O. Kuksenok, L. D. Zarzar, A. Shastri, A. C. Balazs, J. Aizenberg, *Nature* **2012**, *487*, 214.
[31] A. Shastri, L. M. McGregor, Y. Liu, V. Harris, H. Nan, M. Mujica, Y. Vasquez, A. Bhattacharya, Y. Ma, M. Aizenberg, O. Kuksenok, A. C. Balazs, J. Aizenberg, X. He, *Nat. Chem.* **2015**, *7*, 447.
[32] U. S. Schubert, C. Eschbaumer, *Angew. Chem., Int. Ed.* **2002**, *41*, 2892.
[33] S. Hohloch, D. Schweinfurth, M. G. Sommer, F. Weisser, N. Deibel, F. Ehret, B. Sarkar, *Dalton Trans.* **2014**, *43*, 4437.
[34] S. Wanniarachchi, B. J. Liddle, B. Kizer, J. S. Hewage, S. V. Lindeman, J. R. Gardinier, *Inorg. Chem.* **2012**, *51*, 10572.
[35] M. Aizenberg, D. Milstein, *J. Chem. Soc. Chem. Commun.* **1994**, 411.
[36] P. A. Lay, A. M. Sargeson, H. Taube, M. H. Chou, C. Creutz, in *Inorganic Syntheses*, Vol. *24*, (Ed: J. M. Shreeve), John Wiley & Sons, Inc., Hoboken, NJ, USA **2007**, p. 291.
[37] L. McDonald, *Undergraduate Review*, Vol. *4*, Bridgewater State College, **2008**, p. 51, http://vc.bridgew.edu/undergrad_rev/vol4/iss1/1.
[38] V. V. Pavlishchuk, A. W. Addison, *Inorg. Chim. Acta* **2000**, *298*, 97.
[39] N. A. F. Al-Rawashdeh, S. Chatterjee, J. A. Krause, W. B. Connick, *Inorg. Chem.* **2014**, *53*, 294.
[40] K. B. Yatsimirskii, L. P. Tikhonova, *Coord. Chem. Rev.* **1985**, *63*, 241.
[41] S. Hirotsu, Y. Hirokawa, T. Tanaka, *J. Chem. Phys.* **1987**, *87*, 1392.
[42] H. Mihara, Y. Tanaka, T. Fujimoto, N. Nishino, *J. Chem. Soc. Perkin Trans. 2*, **1995**, 1133.
[43] H. F. M. Nelissen, M. C. Feiters, R. J. M. Nolte, *J. Org. Chem.* **2002**, *67*, 5901.
[44] O. Shimomura, B. S. Lee, S. Meth, H. Suzuki, S. Mahajan, R. Nomura, K. D. Janda, *Tetrahedron* **2005**, *61*, 12160.
[45] X. Y. Li, J. Illigen, M. Nieger, S. Michel, C. A. Schalley, *Chem. - Eur. J.* **2003**, *9*, 1332.
[46] A. L. Gerschuns, A. A. Pawljuk, *Ukr. Khim. Zh. (Russ. Ed.)* **1963**, *30*, 955.
[47] R. Docherty, F. Tuna, C. A. Kilner, E. J. L. McInnes, M. A. Halcrow, *Chem. Commun.* **2012**, *48*, 4055.
[48] G. Sheldrick, *Acta Crystallogr., Sect. A* **2008**, *64*, 112.
[49] O. V. Dolomanov, L. J. Bourhis, R. J. Gildea, J. A. K. Howard, H. Puschmann, *J. Appl. Crystallogr.* **2009**, *42*, 339.

